

Rotational Properties of Inverted Hybrid Stars

Rodrigo Negreiros,^{1,2,*} Chen Zhang,³ and Renxin Xu⁴

¹*Catholic Institute of Technology*

1 Broadway - 14th floor, Cambridge, MA 02142

²*Instituto de Física, Universidade Federal Fluminense
- Av. Litoranea - Niteroi - RJ - BR*

³*The HKUST Jockey Club Institute for Advanced Study,*

The Hong Kong University of Science and Technology, Hong Kong SAR, People's Republic of China

⁴*Department of Astronomy, School of Physics, Peking University, Beijing 100871, People's Republic of China*

(Dated: July 10, 2024)

We study the rotational properties of inverted hybrid stars (also termed cross stars), which have been recently proposed as a possible new class of compact stars characterized by an outer layer of quark matter and a core of hadrons, in an inverted structure compared to traditional hybrid stars. We analyze distinct models representing varying depths of quark-hadron phase transitions. Our findings reveal that, while cross stars rotating at their Kepler frequencies typically exhibit a significantly higher mass and larger circumferential radius as anticipated, interestingly, there is a significant increase in potential twin configurations in the case of rapid rotations. We further study sequences of constant baryonic mass, representing potential paths of rotational evolution. Our results indicate that not all stars in these sequences are viable due to the onset of phase transitions during spin-down, leading to possible mini-collapses. We also investigate the phenomenon of “back-bending” during spin-down sequences, which is manifested in a rather different shape for cross stars due to their inverted structure and the large density discontinuity caused by the strong phase transition, in contrast to traditional hybrid stars. Our research enriches existing studies by introducing the significant aspect of rotation, unveiling intriguing phenomena that could serve as observational markers.

I. INTRODUCTION

The concept of phase transitions within compact stars is a very realistic possibility that has been seriously considered for decades [1–8]. Typically, based on our understanding of the baryonic matter phase diagram, the transition from hadronic matter (HM) to deconfined quark matter (QM) at some point within the compact object is considered, with the precise point of this transition is contingent upon the equation of state (EOS) of both the hadronic and quark phases [9–15]. A significant challenge in the study of hybrid stars is determining the hadronic-quark matter transition at the low temperatures typical of compact stars. Furthermore, it remains to be conclusively determined whether the transition occurs at the densities found within the interiors of neutron stars, although it has been suggested that this is probable [16]. Compact stars that undergo a phase transition to quark matter at inner regions are commonly referred to as hybrid stars.

Recently, the provocative possibility of “inverted” hybrid stars was proposed and examined [17, 18]. These objects are composed of an outer layer of quark matter, with the inner stellar region composed of ordinary hadronic matter, in opposite to what one expects for traditional hybrid stars, hence the name “inverted” hybrid stars or cross stars (CrSs) considering that the inverted phase transition occurs when the chemical potentials of

the two matter phases cross. This concept is supported by the hypothesis of absolutely stable QM at low pressure, as demonstrated by [19] for strange quark matter (SQM) that is composed of a nearly equal number of u , d , s quarks, and [20] for up-down quark matter (ud QM) that composed of u , d quarks, together with the possibility that at high pressures hadronic matter may be more stable than QM due to a smaller chemical potential in a large physical EOS parameter space [17]. This inverted phase transition cannot be excluded since it resides in the intermediate density and low-temperature regime where the QCD dynamics is non-perturbative and lattice calculation suffers from the fermion sign problem. Besides, as [17] observed, composition with ud QM allows a larger parameter space than those with SQM. As SQM can form strange quark stars, ud QM can also form up-down quark stars [21–27]. CrSs can be seen as configurations in which a hadronic core developed inside these quark stars.

The properties of non-rotating (spherically symmetric) CrSs have been thoroughly examined in [17], with a focus on their macroscopic features such as mass and radius. This study also explored key quantities for potential merger scenarios, including tidal deformability. Later, the asteroseismology of CrSs was systematically studied in [18]. Building on the findings of [17], our current research delves deeper into the attributes of these objects, with a particular emphasis on the properties of rotating cross stars. The characteristics of rotating compact stars have garnered significant interest recently, particularly due to the potential emergence of high-angular momentum compact stars from merger events. We argue that an in-depth study of rotating CrSs is justified, as it

* rnegreiros@id.uff.br

could yield valuable insights for future dynamic simulations of post-merger remnants, in addition to its inherent scholarly value.

This paper is organized as follows: Section I introduces the context and purpose of this work; Section II provides an overview of the microscopic model used in this study; Section III discusses our findings on the structure of rotating cross stars; Section IV explores potential evolutionary sequences of rotating stars; Section V describes the back-bending phenomena as observed in rotating cross stars; and Section VI offers our conclusions and future perspectives. In this paper, we adopt units where $G = c = 1$.

II. MICROSCOPIC MODEL

In this study, we adopt the methodology of [17] and explore the concept of CrSs, which are theorized to be composed of quark matter at lower densities and hadronic matter at higher densities. As discussed in the introduction, we focus on the CrSs with $udQM$, which has the grand potential expressed as follows:

$$\Omega = -\frac{\xi_4 a_4}{4\pi^2} \mu^4 + B, \quad (1)$$

where μ is the average quark chemical potential. This can be understood as the grand potential of a free quark gas with QCD corrections parameterized by the parameter a_4 , with $a_4 = 1$ signifying no corrections and larger values of a_4 denoting larger corrections [28]. B is the effective bag constant. The parameter ξ_4 for $udQM$, is given by [17] $\xi_4 = [(1/3)^{4/3} + (2/3)^{4/3}]^{-3} \approx 1.86$.

From the potential given in Eq. (1) we can write the following equations for the energy per baryon of $udQM$ [25]

$$(E/A)_q = \frac{3\sqrt{2\pi}}{(a_4 \xi_4)^{1/4}} B^{1/4}, \quad (2)$$

while the equation of state (EOS) is given by

$$P = \frac{\epsilon - 4B}{3}, \quad (3)$$

with ϵ denoting the energy density.

The $udQM$ parameters must be defined within the $udQM$ hypothesis. As discussed in [17] we must take into account the absolute stability condition of QM at zero pressure, which constrains (B, a_4) via $(E/A)_q < 930$ MeV, the energy per baryon number for most stable nucleus ^{56}Fe . Therefore, following in the footsteps of [17], we consider the following benchmark values for the bag constant $B = 20, 35, 50$ MeV/fm³ with the corresponding values of $a_4 = 0.35, 0.62, 0.88$, respectively. Each pair of values for parameters B and a_4 will be denoted, heretofore as parameters set A, B, C. Explicitly, set A corresponds to $B = 20$ MeV/fm³ and $a_4 = 0.35$, set B to

$B = 35$ MeV/fm³ and $a_4 = 0.62$, and set C to $B = 50$ MeV/fm³ and $a_4 = 0.88$.

In the study of CrSs, it is necessary to consider a hadronic EOS. The authors of [17, 18] performed a comprehensive examination of a representative set of hadronic equations of states, which revealed similar qualitative features and small quantitative differences (for details, see their appendices). Consequently, following their observations, in this work we consider the APR EOS [29] for the hadronic sector, as sourced from the ComPOSE database [30]. Employing the $udQM$ hypothesis, as well as the aforementioned hadronic EOS, quark matter transits to hadronic matter as pressure increases beyond the transition pressure P_{cr} as determined by the crossing of the chemical potentials of the two matter phases. The combined EOS for each benchmark model of CrSs is shown in Fig. 1.

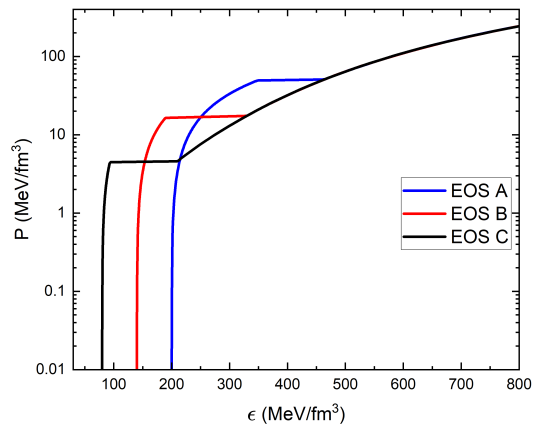


Figure 1: The EOS for cross stars involves $udQM$ transitioning to hadronic matter (APR model) at high pressure. Parameter sets A, B, and C represent varying values for the $udQM$ bag constant and the a_4 parameter. Specifically, set A corresponds to $B = 20$ MeV/fm³ and $a_4 = 0.35$, set B to $B = 35$ MeV/fm³ and $a_4 = 0.62$, and set C to $B = 50$ MeV/fm³ and $a_4 = 0.88$.

III. STRUCTURE OF ROTATING STARS

The structure of rotating neutron stars presents a significantly more complex problem to solve compared to their non-rotating counterparts. For non-rotating, spherically symmetric neutron stars, the combination of Einstein's equation and the equilibrium condition yields the renowned Tolman-Oppenheimer-Volkoff Equations (TOV) [31, 32].

However, the complexity escalates when rotation is introduced into the equation. This is primarily due to the absence of an external, analytical solution for the exterior of a rotating neutron star. This contrasts with the case of spherically symmetric stars, where Birkhoff's theorem demonstrates that the external solution aligns with

Schwarzschild's solution for a point mass.

In the case of a rotating neutron star, it becomes necessary to solve Einstein's equation across all space, applying the appropriate boundary conditions at infinity. For a rotating star exhibiting axial symmetry around its rotation axis, we select a metric that maintains the requisite symmetry. The metric is given by

$$\begin{aligned}
 ds^2 &= g^{\mu\nu} dx_\mu dx_\nu = \\
 &= -e^{\gamma+\rho} dt^2 + e^{2\alpha} (dr^2 + r^2 d\theta^2) \\
 &+ e^{\gamma-\rho} r^2 \sin^2 \theta (d\phi - \omega dt)^2,
 \end{aligned} \quad (4)$$

where the metric functions ρ, γ, α and ω are function of r and θ only. The metric function ω represents the frame dragging frequency, i.e. the frequency at which the local inertial frames are rotating.

The sources of curvature are specified in the energy-momentum tensor. We treat neutron star matter as a perfect fluid in which case the energy-momentum tensor is given by

$$T^{\mu\nu} = (\epsilon + P)u^\mu u^\nu + P g^{\mu\nu}, \quad (5)$$

where ϵ is the energy density, P is the pressure, and u^μ is the four-velocity.

The field equations of the metric functions are obtained by substituting the metric (4) and the energy-momentum tensor (5) into Einstein's field equation

$$G^{\mu\nu} = R^{\mu\nu} - \frac{1}{2}g^{\mu\nu} = 8\pi T^{\mu\nu}, \quad (6)$$

where $R^{\mu\nu}$ is the Riemann curvature tensor.

To find the stellar structure one must solve Eq. (6) in addition to the hydrostatic equilibrium condition, which can be obtained from imposing conservation of momentum-energy ($T^{\mu\nu}{}_{;\mu} = 0$), yielding

$$dP - (\epsilon + P)[d \ln u^t + u^t u_\phi d\Omega] = 0, \quad (7)$$

where Ω is the matter's angular velocity. For rigid rotations, as in this paper, one has $d\Omega = 0$.

These equations must then be solved in all space, with flat space at infinity as boundary conditions. In this work we employ the code *Astreaus*, which has been widely used to study rotating neutron stars [33–37]. This code employs the numerical method described in [38] and have been thoroughly explored in [39].

We show in Fig. 2 the mass as a function of the central density corresponding to the three different EOSs for CrSs that we have considered.

For each EOS examined, we present two curves: one representing the spherical sequence with non-rotating stars (TOV solution), and the other depicting the Kepler sequence where each star rotates at its maximum (Kepler) frequency, that is, the highest frequency before the onset of mass shedding in stars.

The findings illustrated in Fig. 2 reveal that CrSs undergoing a transition from quark matter to hadronic matter at lower densities tend to exhibit smaller masses.

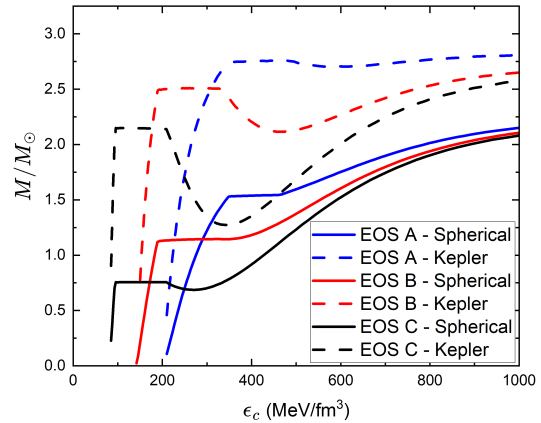


Figure 2: Mass as a function of central density is depicted for three different Equations of State (EOS) of compact stars (CrSs) studied. For each EOS, two curves are presented, represented by solid and dashed lines, corresponding to the spherical sequence where stars have no rotation, and the Kepler sequence where each star rotates at its maximum (Kepler) frequency, respectively.

Conversely, transitions occurring at higher densities result in larger masses.

As anticipated, the impact of rapid rotation is significant, with stars that rotate at the Kepler frequency exhibiting considerably higher mass than their non-rotating counterparts.

It is also worth noting the emergence of twin star configurations, especially for CrSs where the transition occurs at lower densities. Twin star configurations refer to scenarios where two stable stars from the same family have identical mass but differ in central densities (and radii), resulting in varying compactness [40–42]. Typically, twin star setups involve the star with the smaller central density (less compact) being purely hadronic, while its more compact counterpart is hybrid. However, the case of inverted hybrid stars has the reversed situation, where the less compact twin is composed solely of quark matter, and the more compact twin contains both quark matter and hadronic matter, as explicitly shown in [17] for non-rotating CrSs. Here our new finding reveals that, when rotation is introduced, an intriguing phenomenon emerges: the twin branch significantly expands. This is particularly noteworthy in the case of EOS B, where a relatively pronounced twin branch appears when rotation is factored in. This phenomenon may also appear in traditional hybrid stars. For instance, Ref. [43] showed that adding rotations can introduce twin stars from normal stars.

The emergence of twin-star configurations becomes more pronounced when examining the Mass-Radius diagram for these CrS sequences. These findings are depicted in Figures 3, which display the gravitational mass as a function of the circumferential radius. The cyan-shaded region denotes the twin-star configurations. The

insets in these figures illustrate the twin configurations for the corresponding non-rotating ones of the same EOS.

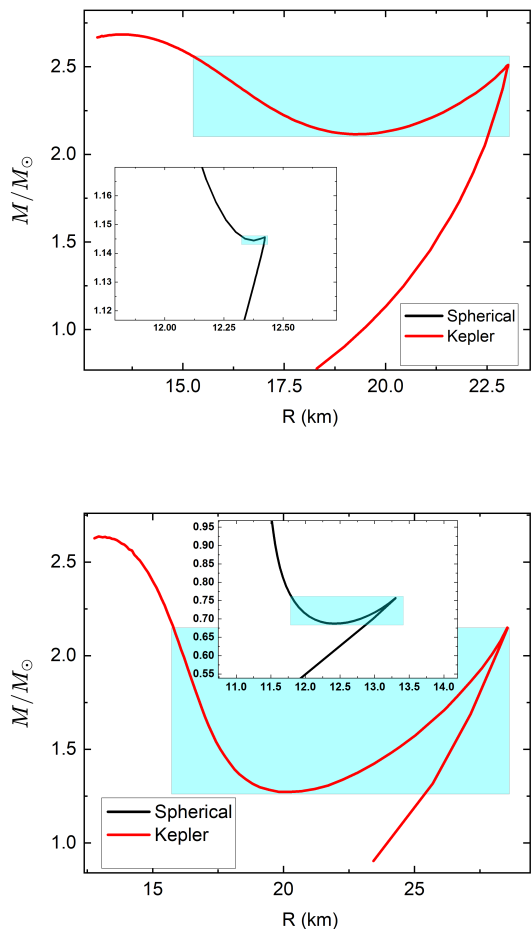


Figure 3: The mass as a function of circumferential radius for CrSs of EOS B (top panel) and EOS C (bottom panel) rotating at their Kepler frequencies. The blue shaded area denotes the zone where twin configurations occur. The insets illustrate the twin configurations of corresponding spherically symmetric (non-rotating) stars.

The findings outlined in Figures 3 highlight a marked increase in twin configurations. The non-rotating scenario reveals minimal twin configurations, while the Kepler frequency sequence exhibits a broad spectrum of twin stars. Even though the Kepler sequence represents an extreme case, there are also intermediate scenarios, underscoring that the inclusion of angular momentum can promote the emergence of twin configurations.

IV. EVOLUTION SEQUENCES

Given that a compact star may be born with a specific angular momentum, whether after a supernova or

a merger event, exploring potential rotational evolution paths as they decelerate is warranted. This involves examining the evolution of a sequence with constant baryon mass from a state of high rotation to the non-rotating limit. Such sequences can reveal the potential evolutionary trajectories of isolated stars that decelerate without mass loss or gain, thereby preserving a constant baryonic mass.

To illustrate such sequences, we show in Fig. 4 the mass as a function of circumferential radius for three sequences of stars with constant baryonic mass, namely $M_B = 1.80, 2.05, 2.31$ and $2.55 M_\odot$, as well as the spherical and Keplerian families for EOS B, with the gray shaded region depicting the forbidden region above the Keplerian sequence. These sequences illustrate possible paths taken by stars with constant baryonic mass, i.e. without losing or gaining matter, as they spin down from a high angular momentum configuration (up to the limit set by the Kepler sequence) to a non-rotating configuration represented by the spherical sequence. The findings across the various EOSs examined are observed to be qualitatively consistent. This implies that all the studied EOSs display the same characteristics. To prevent an overload of figures, we have chosen to illustrate only the results for EOS B, hence, only the results for EOS B are illustrated to avoid an excessive number of figures.

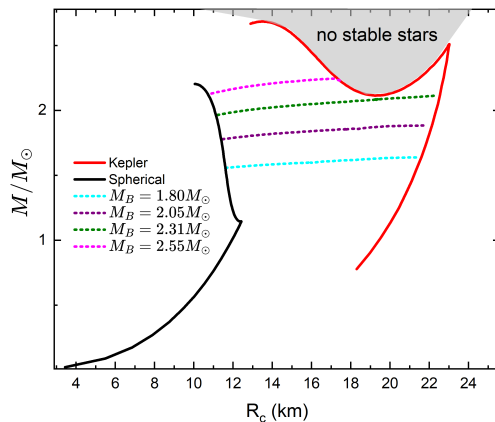


Figure 4: Gravitational mass as a function of circumferential radius for CrSs of EOS B. Each dashed curve represents evolution paths for stars with the indicated baryon mass. The gray-shaded region depicts the forbidden region above the Kepler sequence.

It is crucial to note that while the stars depicted by the constant baryonic sequences in Fig. 4 are hydrostatically stable, not all may be stable against oscillations. The stability condition for a sequence of stars with constant baryonic mass follows the turning point theorem (see for instance [44]) and can be written as

$$\left. \left(\frac{\partial J}{\partial \epsilon_c} \right) \right|_{M_b = \text{const.}} < 0, \quad (8)$$

where J is the angular momentum and ϵ_c the central energy density. Besides the aforementioned condition, it is also necessary to consider the energy density gap in the EOS, which is evident in Fig. 1, resulting from the phase transition.

Taking into account these two constraints, we illustrate in Fig. 5 the relationship between angular momentum and central density for the three constant baryonic mass sequences depicted in Fig. 3. In these figures, we highlight the forbidden regions, as defined by the condition (8), and the prohibited region resulting from the phase-transition gap.

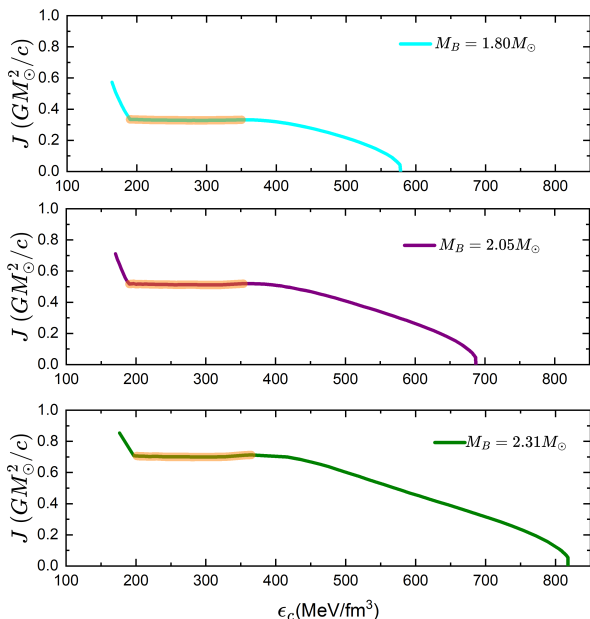


Figure 5: Angular momentum as a function of central density for the constant baryonic mass sequences indicated. The orange highlighted region represents forbidden either due to the phase transition gap and/or stability criteria for constant baryon mass sequences.

We can now achieve a better understanding of the potential evolutionary paths of stars with constant baryonic mass by analyzing such sequences in the mass versus central density diagram depicted in Fig. 6.

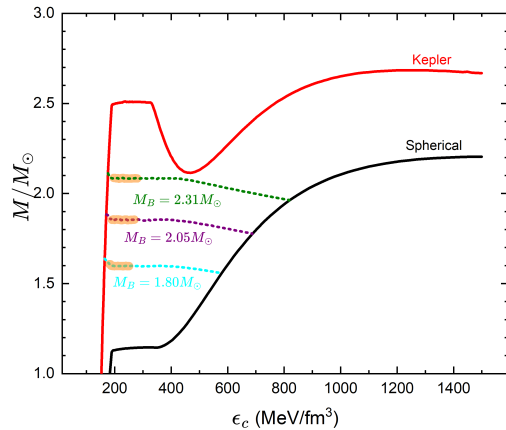


Figure 6: Gravitational mass as a function of central density for the sequence of stars of EOS B. Orange shaded regions represent forbidden configurations.

As observed in Fig. 6, there exists a small region of unstable configuration near to the Kepler sequence. This suggests that stars may originate at lower frequencies (beyond the orange-shaded regions). Alternatively, if they are born with frequencies close to the Kepler limit, they will experience a sudden transition through the prohibited region. A more detailed analysis of the constant baryonic mass curves can provide a better understanding of this phenomenon, which can be facilitated with the aid of Fig. 7

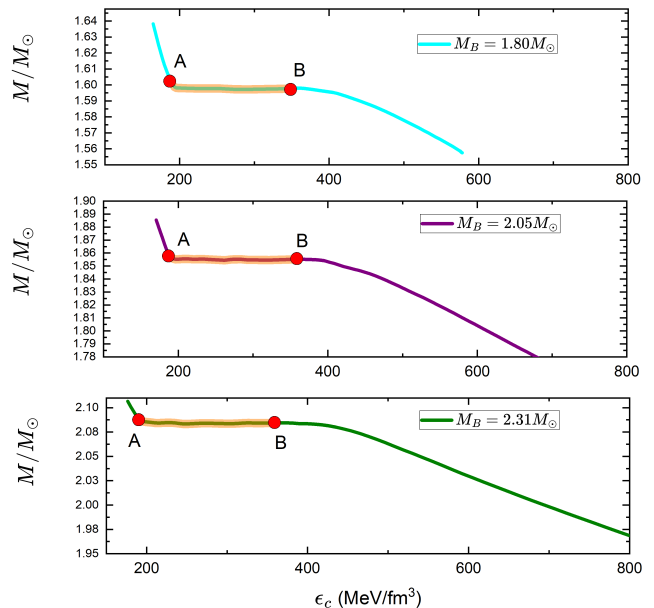


Figure 7: Similar to Fig. 6, but with a zoomed-in region for each of the constant baryonic mass sequences. Points A and B in each figure denote the last stable configuration before and after the forbidden region.

Fig. 7 exhibits a closer look at the constant baryonic mass sequences of Fig. 6. It also indicates two points, A and B , which represent the two stable configurations at the boundary of the forbidden regions. Any star whose initial configuration is before point A , will undergo a fast transition from point A to B . This must be an exothermic process, as the star will lose gravitational mass (mostly due to angular momentum loss) in such a process as $M_B < M_A$. This difference of energy must be partly released as electromagnetic and/or gravitational radiation, whereas the rest will act as heating.

Considering that baryonic mass is constant for the sequences under consideration, we can easily estimate the amount of energy released when a star goes from point A to point B as

$$E_g = M_g^A - M_g^B, \quad (9)$$

where E_g is the energy released, M_g^A and M_g^B are the gravitational mass at points A and B , respectively. Taking the sequence of $M_B = 1.80 M_\odot$ for instance, we obtain

$$E_g \approx 2.4 \times 10^{-3} M_\odot \approx 4.3 \times 10^{51} \text{erg}. \quad (10)$$

A similar result was outlined in reference [44]. One must bear in mind, however, that not all of this energy is to be radiated away, as part of the energy will remain in the star in the form of heat. Even if only 1% of the energy is radiated it could give rise to very energetic phenomena such as gamma-ray bursts and fast-radio bursts [45], thus warranting further investigations on the dynamics of such phenomena.

V. BACK-BENDING

A typical manifestation of the possibility of a phase transition in the core of neutron stars is the phenomena known as “back-bending” [44]. This phenomenon can be comprehended by considering the star’s contractions during its rotational evolution, which reduces the moment of inertia, in conjunction with the softening of the EOS that accompanies the phase transition. These combined factors lead to an increase in the star’s rotational frequency, despite a reduction in its total angular momentum during spin-down. This behavior can be distinctly identified by introducing an additional axis, representing the rotational frequency, to Fig. 6. The resulting graphic, depicted in Fig. 8, clearly demonstrates an increase in rotational frequency corresponding to an increase in stellar

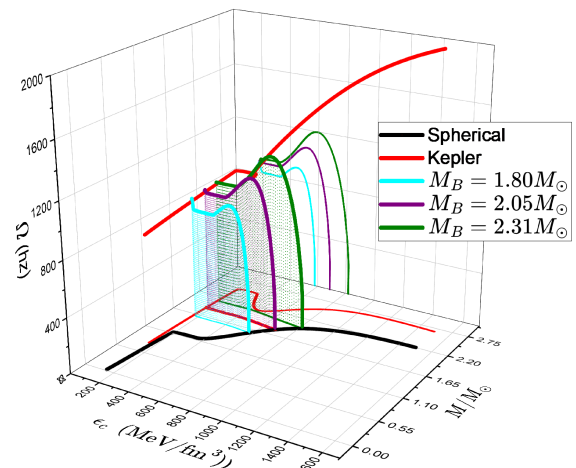


Figure 8: 3D representation of the stellar sequences shown in Fig. 6, with the z -axis representing the rotational frequency.

The increase in frequency illustrated in Fig. 8 is associated with the so-called back-bending, which can be observed when the angular momentum is plotted against the frequency, as can be seen in Fig. 9

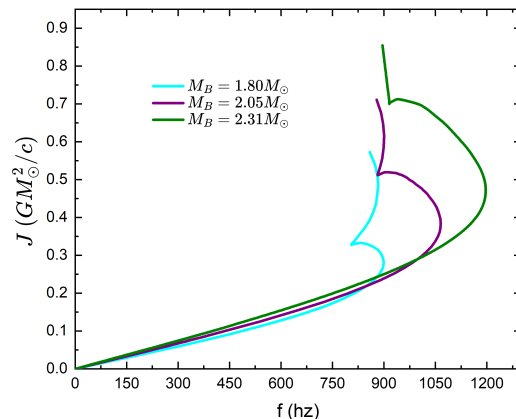


Figure 9: Angular momentum as a function of frequency for constant baryonic mass sequences of EOS B.

The results depicted in Fig. 9 exhibit intriguing behavior. While they retain the expected properties associated with the previously studied back-bending phenomenon (an increase in rotational frequency corresponding to a decrease in angular momentum), the shape of the J - Ω curve is markedly different. Traditional back-bending curves typically display an ‘S’ shape, hence the name ‘back-bending’. However, for the cross stars studied here, we observe a much sharper bend in the curve, more akin to a ‘back-kink’. We attribute this behavior to the nature of the inverted hybrid stars under study and the abrupt density change in nature when the low-pressure ud QM transitions to hadronic matter at higher

pressures. Although we currently have limited observational data regarding the angular momentum of compact stars, future observations of this nature could potentially provide empirical evidence for the model studied here.

VI. CONCLUSIONS

In this research, we built upon the work of [17, 18, 20] which has put forth the intriguing possibility that quark matter can be more stable than hadronic matter at low pressure and be less stable at higher pressure. This provocative possibility gives rise to inverted hybrid stars or cross stars (CrSs) by other names, in which their outer layer is composed of quark matter while the higher-density core is made of hadrons, wherein the quarks are confined.

The studies presented in [17, 18] comprehensively examine the characteristics of cross stars, such as mass, radius, tidal deformability, and oscillations. Our research aims to extend their findings by investigating the attributes of rotating CrSs, including the potential evolutionary trajectories of objects with constant baryonic mass. We find that such studies are garnering renewed interest, especially considering the possibility of post-merger objects with high angular momentum. We have then analyzed three benchmark models for CrSs, each representing a different “depth” of the *ud*QM to hadronic matter phase transition: deep (EOS A), intermediate (EOS B), and shallow (EOS C). All equations of state presuppose the APR EOS for the hadronic matter. We have computed various families of rotating neutron stars across all models to gain a comprehensive understanding of their properties.

Our research reveals that CrSs rotating at their Kepler frequencies typically exhibit a higher mass and a larger circumferential radius, as anticipated. We have also observed an interesting behavior regarding twin configurations, where twin stars are compact objects with identical mass but differing radii, a characteristic often observed in hybrid stars. Our results indicate that in configurations with high angular momentum, such as those in the Kepler sequence, the likelihood of potential twin configurations increases significantly. Moreover, EOS B and EOS C start to exhibit twin stars within their Kepler sequences, despite not presenting such configurations in the non-rotating case.

We have also devoted considerable effort to studying sequences of constant baryonic mass. These sequences are characterized by different stellar configurations that share the same baryonic mass but exhibit varying angular momentum. These configurations reach their extremes at the Kepler sequence, beyond which no hydrostatically stable configurations exist, and at the spherical sequence, which represents the minimum possible angular momentum. Sequences of constant baryonic mass between these two extremes represent potential paths of rotational evolution that stars may follow as they transition from high

angular momentum to spherical, non-rotating configurations. We have shown that although we find a sequence of constant baryon mass connecting stars at the Kepler frequency to their non-rotating counterparts, not all stars in these sequences are viable. While all of them satisfy the hydrostatic equilibrium conditions, some of them are not stable against oscillations. These unstable configurations occur due to the onset of phase transition during the spin-down, which happens as the central density increases during the spin-down, triggering the phase transition within the star. This leads to the possibility of a mini-collapse, occurring in the spin-down of stars with high angular momentum, such as those studied in Ref. [44]. We have estimated that for the current model, these mini-collapses are associated with the release of $\sim 10^{50}$ erg of energy, part of which would be released in the form of electromagnetic and/or gravitational radiation.

We have further investigated the properties of constant baryonic mass during spin-down sequences, particularly the phenomena of “back-bending”. This phenomenon is characterized by an increase in rotational frequency that coincides with a reduction in angular momentum for stars nearing the onset of phase transition. Typically observed in stars undergoing phase transition during spin-down, this phenomenon arises from the need for a rapid increase in rotational frequency to compensate for a substantial decrease in the moment of inertia during the phase transition. This is usually manifested as an ‘S’ shape in the angular momentum graph. However, due to the unique nature of CrSs, which have a quark phase in the outer layers, the back-bending for these stars is exhibited in a rather distinctive way, behaving more akin to what can be described as a ‘back-kink’ due to its sharp shape. Although admittedly remote given our limited observational data on the angular momentum and moment of inertia of neutron stars, there may be a possibility of distinguishing between CrSs and ordinary hybrid stars if more observational data on the relevant quantities become available in the future.

With this work, our objective has been to build upon previous studies of inverted hybrid stars by incorporating the significant aspect of rotation. Our research has unveiled intriguing phenomena that occur in this new type of compact star when angular momentum is taken into account, some of which could potentially serve as observational markers with the emergence of new data. We believe that our work enriches the studies presented by [17, 20], introducing an additional and captivating layer of complexity. We intend to delve deeper into the fascinating concept of CrSs by investigating differential rotation and magnetic fields, a study that is currently in progress and will be detailed in our future works.

ACKNOWLEDGMENTS

R.N. acknowledges financial support by FAPERJ under project Proc. No. E-26/201.432/2021. R.N. extends

his gratitude to Prof. Renxin Xu for the warm hospitality and pleasant atmosphere provided during the visit to PKU in October 2023. C. Z. is supported by the Jockey Club Institute for Advanced Study at The Hong Kong University of Science and Technology.

-
- [1] V. Dexheimer, L. T. T. Soethe, J. Roark, R. O. Gomes, S. O. Kepler, and S. Schramm, *International Journal of Modern Physics E* **27**, 1830008 (2018), <https://doi.org/10.1142/S0218301318300084>.
- [2] M. G. Orsaria, G. Malfatti, M. Mariani, I. F. Ranea-Sandoval, F. García, W. M. Spinella, G. A. Contrera, G. Lugones, and F. Weber, *Journal of Physics G: Nuclear and Particle Physics* **46**, 073002 (2019).
- [3] H. Heiselberg and M. Hjorth-Jensen, *The Astrophysical Journal* **525**, L45 (1999).
- [4] N. K. Glendenning, *Physics Reports* **342**, 393 (2001).
- [5] F. Yang and H. Shen, *Physical Review C* **77**, 025801 (2008).
- [6] S. Reddy, G. Bertsch, and M. Prakash, *Physics Letters B* **475**, 1 (2000).
- [7] N. K. Glendenning, *Physical Review D* **46**, 1274 (1992).
- [8] G. Burgio, M. Baldo, P. Sahu, and H.-J. Schulze, *Physical Review C* **66**, 025802 (2002).
- [9] M. Alford, M. Braby, M. Paris, and S. Reddy, *The Astrophysical Journal* **629**, 969 (2005).
- [10] C. Zhang, Y. Gao, C.-J. Xia, and R. Xu, *Physical Review D* **108**, 123031 (2023).
- [11] M. Cierniak and D. Blaschke, *Astronomische Nachrichten* **342**, 819 (2021).
- [12] G. Peng, A. Li, and U. Lombardo, *Physical Review C* **77**, 065807 (2008).
- [13] D. Blaschke, J. Berdermann, and R. Lastowiecki, *Progress of Theoretical Physics Supplement* **186**, 81 (2010).
- [14] V. Dexheimer, R. Negreiros, and S. Schramm, *The European Physical Journal A* **48**, 1 (2012).
- [15] V. Dexheimer, J. Steinheimer, R. Negreiros, and S. Schramm, *Physical Review C* **87**, 015804 (2013).
- [16] E. Annala, T. Gorda, A. Kurkela, J. Nättilä, and A. Vuorinen, *Nature Physics* **16**, 907 (2020).
- [17] C. Zhang and J. Ren, *Physical Review D* **108**, 063012 (2023).
- [18] C. Zhang, Y. Luo, H.-B. Li, L. Shao, and R. Xu, *Physical Review D* **109**, 063020 (2024).
- [19] E. Witten, *Phys. Rev. D* **30**, 272 (1984).
- [20] B. Holdom, J. Ren, and C. Zhang, *Physical Review Letters* **120**, 222001 (2018).
- [21] C. Zhang, *Phys. Rev. D* **101**, 043003 (2020), [arXiv:1908.10355 \[astro-ph.HE\]](https://arxiv.org/abs/1908.10355).
- [22] J. Ren and C. Zhang, *Phys. Rev. D* **102**, 083003 (2020), [arXiv:2006.09604 \[hep-ph\]](https://arxiv.org/abs/2006.09604).
- [23] C.-J. Xia, S.-S. Xue, R.-X. Xu, and S.-G. Zhou, *Phys. Rev. D* **101**, 103031 (2020), [arXiv:2001.03531 \[nucl-th\]](https://arxiv.org/abs/2001.03531).
- [24] Z. Cao, L.-W. Chen, P.-C. Chu, and Y. Zhou, *Phys. Rev. D* **106**, 083007 (2022), [arXiv:2009.00942 \[astro-ph.HE\]](https://arxiv.org/abs/2009.00942).
- [25] C. Zhang and R. B. Mann, *Physical Review D* **103**, 063018 (2021).
- [26] L. Wang, J. Hu, C.-J. Xia, J.-F. Xu, G.-X. Peng, and R.-X. Xu, *Galaxies* **9**, 70 (2021).
- [27] J. M. Z. Pretel and C. Zhang, (2024), [arXiv:2401.12519 \[nucl-th\]](https://arxiv.org/abs/2401.12519).
- [28] M. Alford, M. Braby, M. Paris, and S. Reddy, *The Astrophysical Journal* **629**, 969 (2005).
- [29] a. Akmal, V. R. Pandharipande, and D. G. Ravenhall, *Physical Review C* **58**, 1804 (1998).
- [30] COMPOSE, <https://compose.obspm.fr>.
- [31] R. C. Tolman, *Physical Review* **55**, 364 (1939).
- [32] J. R. Oppenheimer and G. M. Volkoff, *Phys. Rev.* **55**, 374 (1939).
- [33] R. Negreiros, S. Schramm, and F. Weber, *Astronomy and Astrophysics* **603**, A44 (2017).
- [34] R. Negreiros, S. Schramm, and F. Weber, *Astronomische Nachrichten* **335**, 703 (2014), <https://onlinelibrary.wiley.com/doi/pdf/10.1002/asna.201412096>.
- [35] R. Negreiros, S. Schramm, and F. Weber, *Physics Letters B* **718**, 1176 (2013), [arXiv:1103.3870 \[astro-ph.HE\]](https://arxiv.org/abs/1103.3870).
- [36] R. Negreiros, S. Schramm, and F. Weber, *Physical Review D* **85**, 104019 (2012), [arXiv:1201.2381 \[astro-ph.HE\]](https://arxiv.org/abs/1201.2381).
- [37] R. Negreiros, V. Dexheimer, and S. Schramm, *Physical Review C* **82**, 035803 (2010).
- [38] H. Komatsu, Y. Eriguchi, and I. Hachisu, *Monthly Notices of the Royal Astronomical Society* **237**, 355 (1989).
- [39] N. Stergioulas and J. L. Friedman, *The Astrophysical Journal* **444**, 306 (1995).
- [40] S. Schramm, V. Dexheimer, and R. Negreiros, *The European Physical Journal A* **52**, 1 (2016).
- [41] V. Dexheimer, R. Negreiros, and S. Schramm, *Physical Review C* **91**, 055808 (2015).
- [42] F. Lyra, L. Moreira, R. Negreiros, R. Gomes, and V. Dexheimer, *Physical Review C* **107**, 025806 (2023).
- [43] L. Tsaloukidis, P. S. Koliogiannis, A. Kanakis-Pegios, and C. C. Moustakidis, *Phys. Rev. D* **107**, 023012 (2023), [arXiv:2210.15644 \[astro-ph.HE\]](https://arxiv.org/abs/2210.15644).
- [44] P. Haensel, M. Bejger, M. Fortin, and L. Zdunik, *The European Physical Journal A* **52**, 1 (2016).
- [45] W.-Y. Wang, C. Zhang, E. Zhou, X. Liu, J. Niu, Z. Zhou, H. Gao, J. Liu, R. Xu, and B. Zhang, (2024), [arXiv:2405.07152 \[astro-ph.HE\]](https://arxiv.org/abs/2405.07152).